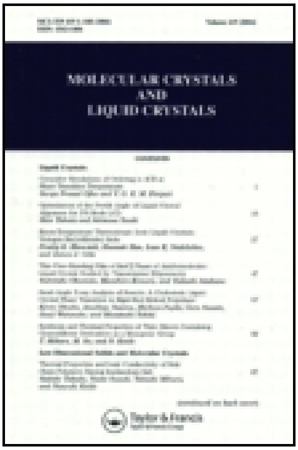

Molecular Crystals and Liquid Crystals

Publication details, including instructions for authors and subscription information:
http://www.tandfonline.com/loi/gmcl20

Induction and Control of Columnar Mesophase by Charge Transfer Interaction and Side Chain Structures of Tetrasubstituted Pyrenes

Takuji Hirose [a], Osamu Kawakami [a] & Mikio Yasutake [a]

[a] Department of Applied Chemistry, Saitama University, Sakura, Saitama, Japan

To cite this article: Takuji Hirose, Osamu Kawakami & Mikio Yasutake (2006): Induction and Control of Columnar Mesophase by Charge Transfer Interaction and Side Chain Structures of Tetrasubstituted Pyrenes, Molecular Crystals and Liquid Crystals, 451:1, 65-74

To link to this article: http://dx.doi.org/10.1080/154214090960081

Mol. Cryst. Liq. Cryst., Vol. 451, pp. 65–74, 2006

ISSN: 1542-1406 print/1563-5287 online
DOI: 10.1080/154214090960081

Induction and Control of Columnar Mesophase by Charge Transfer Interaction and Side Chain Structures of Tetrasubstituted Pyrenes

Takuji Hirose
Osamu Kawakami
Mikio Yasutake
Department of Applied Chemistry, Saitama University,
Sakura, Saitama, Japan

The induction of the columnar phase is described in which intrinsically crystalline 1,4,6,9-tetraacyloxypyrenes have been mixed with tetranitrofluorenone, TeNF, as an electron acceptor. The pyrene derivative with linear nonyl chains, PC_9*, has not shown any mesophases using trinitrofluorenone, suggesting that stronger charge transfer interaction is favored by TeNF. The shape of the substituents works to control the mesophase type: the mixture of* PC_9 *and TeNF has formed a rectangular columnar phase, and a hexagonal columnar phase is attained by rounder derivatives bearing branched side chains.*

Keywords: charge transfer interaction; columnar mesophase; side chain structures; tetranitrofluorenone; tetrasubstituted pyrenes

INTRODUCTION

The organization of molecular materials is attracting a lot of interest. In recent years, self-assembly has been recognized as a powerful method of molecular organization in various fields [1]. Highly organized molecular assembly is important in nanotechnology as well as in biological systems [2]. Various interactions are applied for self-assembly and, among them, π–π interaction is a well known but powerful tool to build up one-dimensional aromatic architecture [3]. In spite of the fact that one-dimensional stacking is a simple architecture, the liquid crystalline (LC) one, an ordered columnar phase, is

Address correspondence to Takuji Hirose, Department of Applied Chemistry, Saitama University, 255 Shimo-ohkubo, Sakura, Saitama 338-8570, Japan. E-mail: hirose@apc.saitama-u.ac.jp

important for various applications [4] due to its anisotropic and thermotropic properties, especially for electronic applications [3b, 5–9]. However, the methodology to intentionally manifest the LC phase has not been well established. Here we report on the induction and control of the columnar mesophase from crystalline pyrene derivatives by taking advantage of the electronic and structural characteristics of 2,4,5,7-tetranitro-9-fluorenone, TeNF [10].

Most discotic compounds showing a columnar phase have large and highly symmetric aromatic cores resulting from high melting temperatures [4–6] and less solubility in common organic solvents [11]. In this study, therefore, we chose pyrene, which has an aromatic core of C_2 symmetry and designed some derivatives to achieve columnar LC phases of lower melting temperatures. As far as we know, only a few simple pyrene derivatives are known to have low melting temperatures [7,8].

RESULTS AND DISCUSSION

The typical synthetic procedure for pyrene derivatives is shown in Scheme 1 [7,12]. Simple crystalline esters $\mathrm{PC_n}$ (n = 8, 9, 11) [7] were prepared with long linear alkyl halides while branched side chains were introduced as $\mathrm{PC_{m.n}}$ (m.n = 3.3, 2.4, 5.5) to reduce the π–π interactions of the central cores. The DSC measurements showed, however, that they were all crystalline and I-Cr transition temperatures were higher for $\mathrm{PC_{m.n}}$ than $\mathrm{PC_n}$ except $\mathrm{PC_{3.3}}$ (Table 1). The transition of $\mathrm{PC_{3.3}}$ at 71°C was expected to be a crystal–crystal one from polarizing optical microscopic (POM) observation. Although the effect of

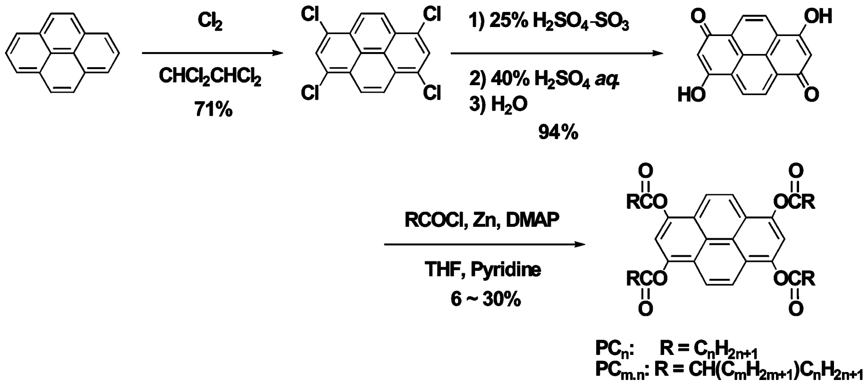

SCHEME 1 Synthesis of tetrasubstituted pyrenes.

TABLE 1 Thermal Properties of PC_n and $PC_{m.n}$

Pyrene derivatives	I		X		Cr
PC_8	●	76 (36.8)	–		●
PC_9	●	67 (49.1)	–		●
PC_{11}	●	72 (46.5)	–		●
$PC_{3.3}$	●	172 (48.1)	●	71 (35.2)	●
$PC_{2.4}$	●	130 (23.5)	–		●
$PC_{5.5}$	●	151 (35.8)	–		●

PC_n: On cooling at 5°C min^{-1}, $PC_{m.n}$: On cooling at 10°C min^{-1}.
I: Isotropic, X: Undetermined, Cr: Crystalline.

branched side chains is ambiguous, Table 1 still shows that they reduce the transition enthalpy about 10 J g^{-1}.

It is known that thermotropic LCs can be formed when 2,4,7-trinitro-9-fluorenone, TrNF [13], is mixed with discotic compounds, which do not show mesomorphism themselves [14–16]. Electron-rich discotic compounds are expected to form charge transfer (CT) complexes with electron-deficient TrNF. In this study, PC_9 and TrNF were mixed in 2:1, 3:2, and 1:1 ratios to obtain a red solid. Although the color change suggested the formation of CT complexes, no mesophases were observed for any mixtures. The interaction between PC_9 and TrNF may not be strong enough to form stable cores for LC phases.

Accordingly, TeNF was prepared [10] to increase the interaction with the pyrene derivatives. The mixture of PC_9 and TeNF gave a dark brown solid in various ratios, suggesting stronger CT interaction than that between PC_9 and TrNF. Their thermal properties were studied with DSC and POM, and the results are summarized in Table 2. Table 2 suggests the LC phase for 2:1 ~ 1:1 PC_9–TeNF mixtures, and they were all Col_r phases as demonstrated by the mosaic and sea grass textures for the 1:1 PC_9–TeNF mixture (Fig. 1). The 4:3 mixture was found to have the most stable LC phase between 67–112°C.

To compare the difference between PC_9-TrNF and PC_9-TeNF, the UV-vis spectra of each 1:1 mixture were measured in the solid state, and they are shown in Fig. 2. Both spectra reach to the visible region (above 450 nm), which proves CT, considering that none of PC_9, TrNF, and TeNF have absorption in the same region. The λ_{max} at longer wavelength (555 nm) for PC_9-TeNF indicated a smaller energy gap between the HOMO of PC_9 and the LUMO of TeNF than that for PC_9-TrNF ($\lambda_{max} = 501$ nm). Higher electron acceptability of TeNF seems to affect the CT from PC_9, making a stable core and leading to the LC phase emergence. The HOMO-LUMO energy gaps were

TABLE 2 Thermal Properties of the Mixtures of PC_9, $PC_{3.3}$, $PC_{2.4}$, and $PC_{5.5}$-TeNF

Pyrene derivatives	PC_n–TeNF ratio	I		Col_r		Col_h		Cr
PC_9	4:1	●	61 (45.9)	–		–		●
	5:3	●	83 (9.0)	●		–	66 (41.5)	●
	4:3	●	112 (19.4)	●		–	67 (27.6)	●
	6:5	●	75 (5.3)	●		–	66 (46.3)	●
	5:5	●[a]	75 (6.6)	–		●[b]	67 (35.4)	●
	5:6	●	56 (35.6)	–		–		●
$PC_{3.3}$	1:1	●		–	138 (5.6)	●	88 (24.9)	●
$PC_{2.4}$	4:3	●		–	102 (5.2)	●	40 (16.7)	●
$PC_{5.5}$	1:1	●		–	156 (5.1)	●	84 (19.1)	●

On cooling at 5°C min^{-1}.

I: Isotropic, Col_r: Discotic rectangular columnar, Col_h: Discotic hexagonal columnar, Cr: Crystalline.

[a] Phase separation of I and Col_h was observed.

[b] Phase separation of Col_h and Cr was observed.

estimated for tetraacetyloxy pyrene, PC_1, TrNF, and TeNF by PM3 molecular orbital calculations [17]. The computations were performed with MM2 and MOPAC 97 programs. The HOMO energy of PC_1 was −7.98 eV and the LUMO energy levels were −2.94 and −3.34 eV for TrNF and TeNF, respectively.

Although all mixtures were crystalline at rt, no single crystals were obtained for the present PCs in Table 1. To obtain structural

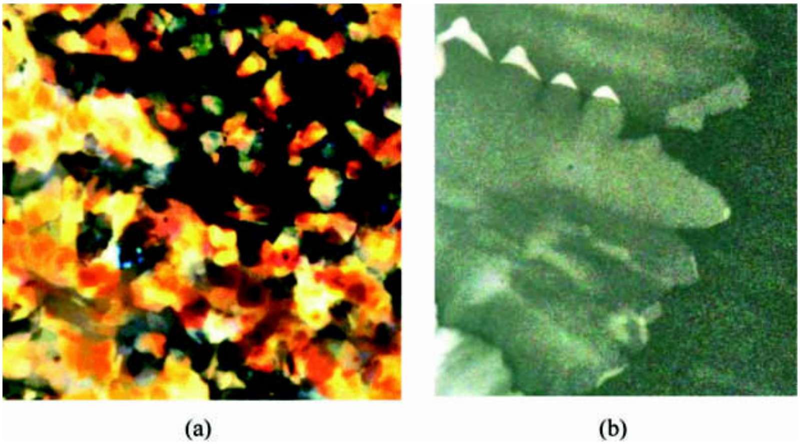

FIGURE 1 Mosaic (a) and sea grass (b) textures of Col_r of PC_9-TeNF (1:1) at 122°C.

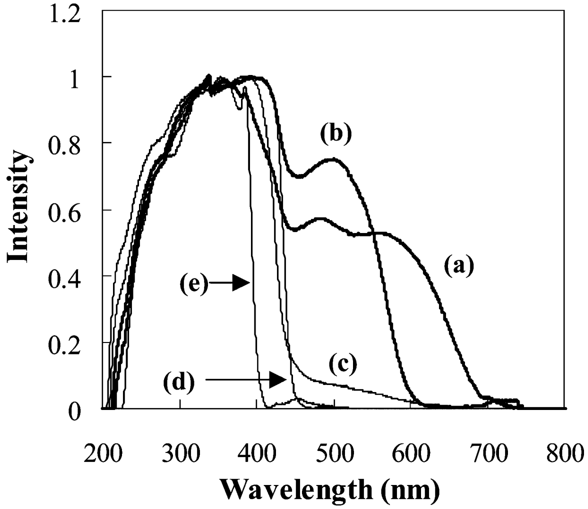

FIGURE 2 UV-vis spectra of (a) PC_9-TeNF (1:1), (b) PC_9-TrNF (1:1), (c) TeNF, (d) TrNF, and (e) PC_9 in their crystalline phases.

information, therefore, PC_1 was prepared, and the mixtures with TrNF and TeNF have colors similar to PC_9-TrNF and PC_9-TeNF. Their single crystals were analyzed by X-ray crystallography and the Ortep diagrams for PC_1-TrNF and PC_1-TeNF are shown in Figs. 3 and 4, respectively.

For PC_1-TrNF, the columnar structure of their rings was formed in a 1:1 ratio with PC_1 and TrNF aromatic rings parallel to each other. The distance was 3.34 Å but TrNF was disordered (Fig. 3). In addition, two characteristics were found: (1) the long axes of PC_1 and TrNF are almost crossed with each other and (2) the center of PC_1 deviated from that of TrNF. These should be due to the asymmetrical charge density of the LUMO. On the other hand, the PC_1-TeNF crystal structure was constructed in a 1:2 ratio, even prepared from the 1:1 mixture. The units were arranged in a zigzag way along the *b* axis direction, and the unit was perpendicular to the neighboring units, as shown in Fig. 4. In addition, three interesting features were observed: (1) the long axes of PC_1 and TeNF are almost eclipsed, but (2) the PC_1 and TeNF rings are not parallel to each other with the center-to-center distance of 3.84 Å, whereas (3) the two TeNF rings are parallel. The symmetrical structure and the four bulky nitro groups of TeNF should be their cause but the reason for the 1:2 composition ratio is unexplained at present.

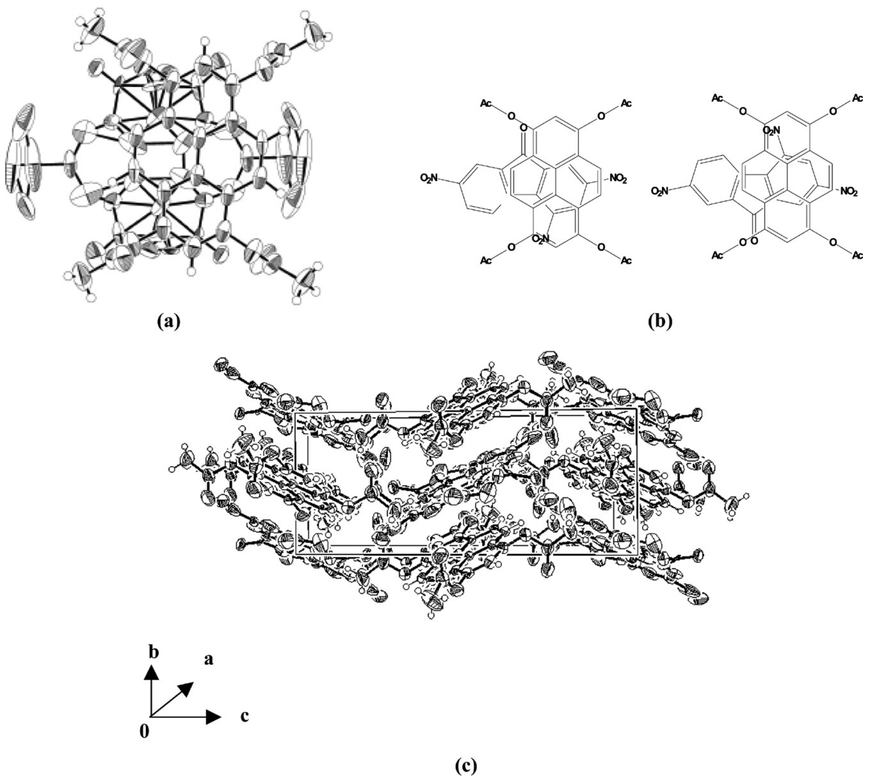

FIGURE 3 Ortep diagram of PC$_9$-TrNF (a) and view showing the frame format of Ortep (b) and crystal packing diagram (c) of the PC$_9$-TrNF (1:2) complex.

Based on the result of PC$_9$, PC$_{5.5}$ with branched side chains was also blended with TeNF. The PC$_{5.5}$:TeNF mixture in a 1:1 ratio was observed to have a hexagonal columnar phase Col$_h$ by POM (Fig. 5). The phase transition behaviors are summarized in Table 2. In the PC$_{m.n}$–TeNF composition range studied, that is, between 2:1 and 2:3, all mixtures of PC$_{2.4}$, PC$_{3.3}$, and PC$_{5.5}$ formed Col$_h$ phases (Table 2).

Table 2 shows a couple of interesting features of PC-TeNF mixtures: (1) the rectangular PC derivative with linear side chains like PC$_9$ formed a Col$_r$ phase (Fig. 6a); (2) rounder PC$_{3.3}$ and PC$_{5.5}$ with branched side chains turned to the Col$_h$ phase (Fig. 6b) with higher transition temperatures; and (3) PC$_{2.4}$, having asymmetrical branches with the same carbon number as PC$_{3.3}$, showed the lowest Col$_h$-Cr transition temperature at 40°C. It is noteworthy that the LC-Cr transition temperatures were higher for all PC$_{m.n}$ with smaller

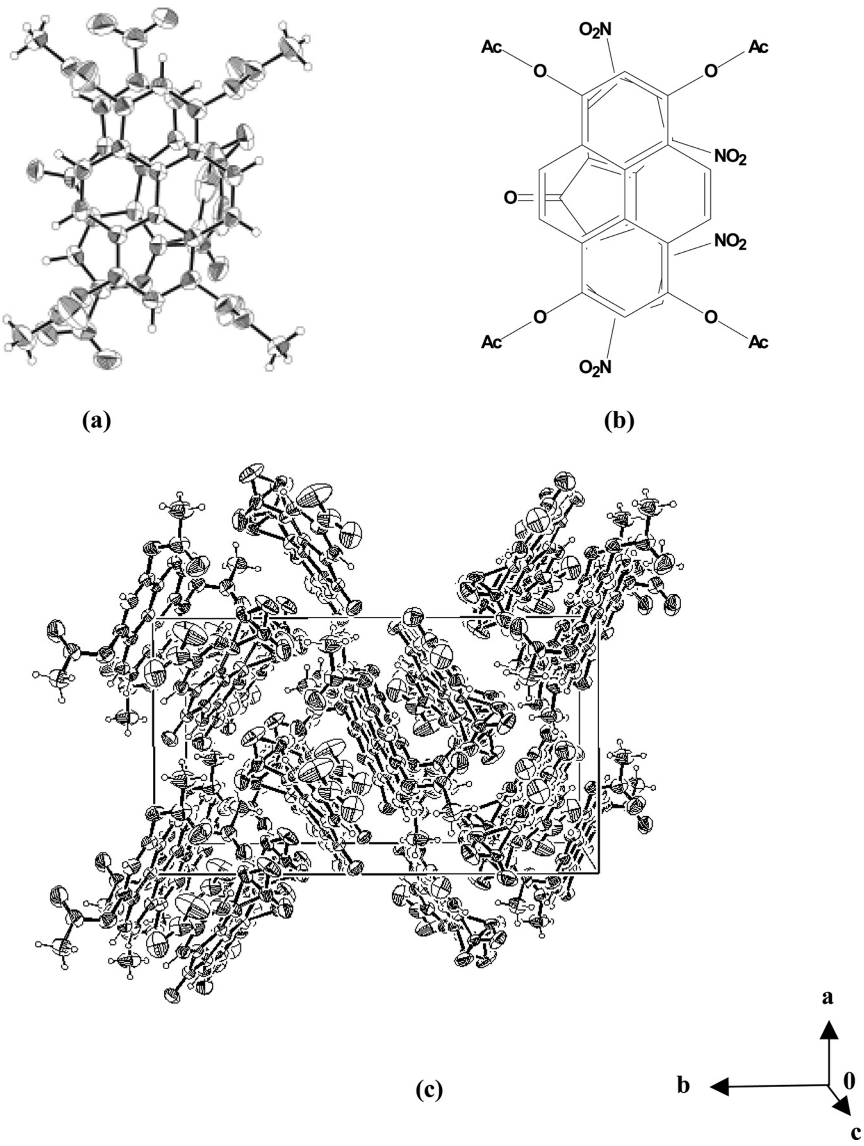

FIGURE 4 Ortep diagram of PC_9-TeNF (a) and view showing the frame format of Ortep (b) and crystal packing diagram (c) of the PC_9-TeNF (1:2) complex.

transition enthalpies than PC_n. It indicates that the side chain structure can control the morphology for the LC phase effectively as presented for porphyrine derivatives by Ohta et al. [18].

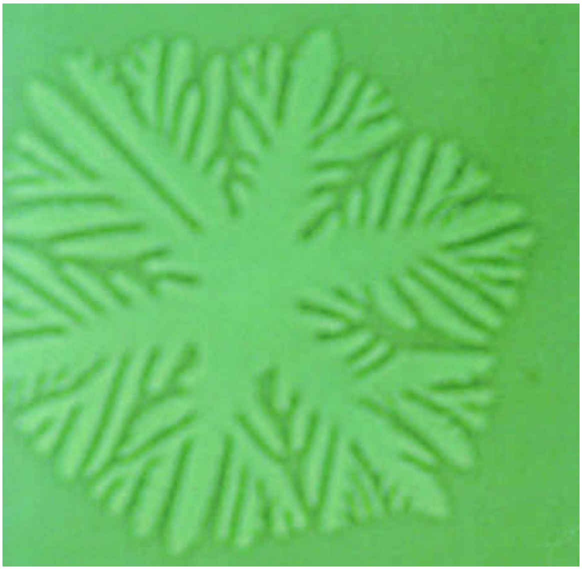

FIGURE 5 Snow-like texture of Col_h of $PC_{5.5}$-TeNF (1:1) at 122°C.

DATA

X-ray crystallographic data of PC_1-TrNF: empirical formula $C_{18.50}H_{11.50}N_{1.50}\ O_{7.50}$; formula weight 374.79; black prisms; crystal dimensions $0.20 \times 0.20 \times 0.30\,mm^3$; monoclinic; space group $P2_1/n$ (#14); $a = 11.855(5)$, $b = 7.770(5)$, $c = 18.721(5)\,Å$, $\beta = 102.907(5)°$,

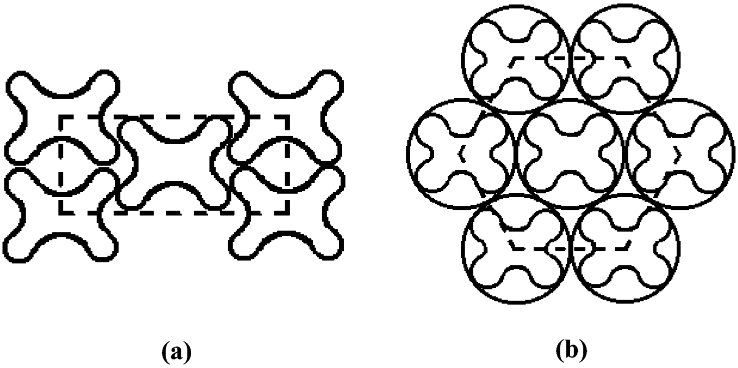

(a) **(b)**

FIGURE 6 Schematic view showing the frame format of rectangular (a) and hexagonal (b) structures of PC derivatives.

$V = 1680.9(14)\,\text{Å}^3$, $Z = 4$; $D_{\text{calcd}} = 1.481\,\text{g/cm}^3$; $F(000) = 772.00$; $\mu(\text{MoK}\alpha) = 0.117\,\text{cm}^{-1}$; $2\theta_{\max} = 55.0°$; no. of reflections measured 3847; no. of observations ($I > 2.00\sigma$ (I), $2\theta < 55.0°$) 3847; no. of variables 338; reflection/parameter ratio was 11.38; $R = 0.0792$; $R_w = 0.1538$; GOF $= 0.841$.

X-ray crystallographic data of PC$_1$-TeNF: empirical formula $C_{25}H_{13}N_4O_{13}$; formula weight 577.39; black prisms; crystal dimensions $0.2 \times 0.3 \times 0.2\,\text{mm}^3$; monoclinic; space group *P2₁/a* (#14); $a = 10.7720(4)$, $b = 18.7790(9)$, $c = 12.4590(5)\,\text{Å}$, $\beta = 90.958(3)°$, $V = 2519.95(18)\,\text{Å}^3$, $Z = 4$; $D_{\text{calcd}} = 1.522\,\text{g/cm}^3$; $F(000) = 1180.00$; $\mu(\text{MoK}\alpha) = 0.126\,\text{cm}^{-1}$; $2\theta_{\max} = 55.0°$; no. of reflections measured 17314; no. of observations ($I > 2.00\sigma$ (I), $2\theta < 55.0°$) 4922; no. of variables 420; reflection/parameter ratio was 11.72; $R = 0.0690$; $R_w = 0.2167$; GOF $= 1.562$.

Crystallographic data (excluding structure factors) for the structures reported in this paper have been deposited with the Cambridge Crystallographic Data Centre as supplementary publications no. CCDC-244511 (PC$_1$-TrNF) and 244510 (PC$_1$-TeNF). Copies of the data can be obtained free of charge upon request to CCDC, 12 Union Road, Cambridge CB2 1EZ, UK [Fax: +44(1223)336033; E-mail: deposit@ccdc.cam.ac.uk].

SUMMARY

Some pyrene derivatives with four acyloxy chains were prepared. Although all of them were crystalline, the addition of TeNF allowed for LC phase emergence caused by CT complexation. It was shown that the LC phase type can be controlled by the structure of the side chain: linear side chains formed Col$_r$ whereas branched ones led to Col$_h$. A more comprehensive study on the LC emergence of PC derivatives is under way, and the relationships with the side chain structure and the LC properties will be reported in the near future.

REFERENCES

[1] Lehn, J.-M. (1995). *Supramolecular chemistry*, VHC: Weinheim, 139.

[2] (a) Cornelissen, J. J. L. M., Rowan, A. E., Nolte, R. J. M., & Sommerdijk, N. A. J. M. (2001). *Chem. Rev.*, *101*, 4039.
(b) Kleppinger, R., Lillya, C. P., & Yang, C. (1997). *J. Am. Chem. Soc.*, *119*, 4097.
(c) Trzaska, S. T. & Swager, T. (1998). *Chem. Mater.*, *10*, 438.

[3] (a) Lifshitz, E., Goldfarb, D., Vega, S., Luz, Z., & Zimmermann, H. (1987). *J. Am. Chem. Soc.*, *109*, 7280.
(b) O'Neill, M. & Kelly, S. M. (2003). *Adv. Mater.*, *15*, 1135.

[4] Borden, N. & Movaghar, B. (1998). Chapter IX application properties of columnar discotic liquid crystals. In: *Handbook of Liquid Crystals*, Demus, D., Goodby, J., Gray, G. W., Spiess, H.-W., & Vill, V. (Eds.), Wiley-VCH: Weinheim, 781.

[5] Adam, D., Schuhmacher, P., Simmer, J., Haussling, L., Siemensmeyer, K., Etzbachi, K. H., Ringsdorf, R., & Haarer, D. (1994). *Nature*, *371*, 141.

[6] (a) Warman, J. M. & Schouten, P. G. (1995). *J. Phys. Chem.*, *99*, 17181.
(b) Warman, J. M. & van de Craats, A. M. (1999). *Adv. Mater.*, *11*, 1469.

[7] Bock, H. & Helfrich, W. (1995). *Liquid Cryst.*, *18*, 707.

[8] Hassheider, T., Benning, S. A., Kitzerow, H.-S., Achard, M.-F., & Bock, H. (2001). *Angew. Chem. Int. Ed. Engl.*, *40*, 2060.

[9] Liu, C.-Y., Fechtenkötter, A., Watson, M. D., Müllen, K., & Bard, A. J. (2003). *Chem. Mater.*, *15*, 124.

[10] Newman, M. S. & Boden, H. (1962). *Org. Synth.*, *42*, 95.

[11] Mullen, K., Spiess, H. W., Fechtenkotter, A., Saalwachter, K., & Harbison, M. A. (1999). *Angew. Chem. Int. Ed. Engl.*, *38*, 3039.

[12] Vollmann, H., Becker, H., Correll, M., & Streeck, H. (1937). *Liebigs Ann. Chem.*, *531*, 1.

[13] Horning, E. C. & Orchin, M. (1955). *Org. Synth.*, *3*, 837.

[14] (a) Ringsdorf, H., Bengs, H., Karthaus, O., Wüstefeld, R., Ebert, M., Wendroff, J. H., Kohne, B., & Praefcke, K. (1990). *Adv. Mater.*, *2*, 141.
(b) Ringsdorf, H., Wüstefeld, R., Zerta, E., Ebert, M., Joachim H., & Wendorff, J. H. (1989). *Angew. Chem. Int. Ed. Engl.*, *7*, 914.

[15] Baehr, C., Evert, M., Frick, G., & Wendorff, J. H. (1990). *Liquid Crystals*, *4*, 601.

[16] Lee, S. & Chang, J. (2003). *Tetrahedron Lett.*, *44*, 7493.

[17] (a) Dewar, M. J. S., Zoebisch, E. G., Healy, E. F., & Stewart, J. J. P. (1985). *J. Am. Chem. Soc.*, *107*, 3902.
(b) Stewart, J. J. P. (1998). *WinMOPAC Ver.2*, Fujitsu Ltd: Tokyo, Japan.

[18] Ohta, K., Yamaguchi, N., & Yamamoto, I. (1998). *J. Mater. Chem.*, *8*, 2637.